Proceedings of Science and Mathematics
Faculty of science, universiti teknologi malaysia
https://science.utm.my/procscimath
Volume 35 (2026) 151-161

Synergistic Antibacterial Effect of *Ficus deltoidea*-Biosynthesized Silver Nanoparticles and Conventional Antibiotics

Xu Duo[a], To Soonwei[a], Nik Ahmad Nizam Nik Malek[a,b]*
[a]Department of Biosciences, Faculty of Science, Universiti Teknologi Malaysia, 81310 UTM Skudai, Johor, Malaysia
[b]Centre for Sustainable Nanomaterials (CSNano), Ibnu Sina Institute for Scientific and Industrial Research (ISI-ISIR), Universiti Teknologi Malaysia, 81310 UTM Skudai, Johor, Malaysia
*Corresponding author: niknizam@utm.my

Abstract
Rising antimicrobial resistance has led to an urgent demand for alternative antibacterial strategies. This research aimed to biosynthesize silver nanoparticles using *Ficus deltoidea* stem extract as a green reducing and stabilizing agent. The AgNPs synthesis parameters were optimized firstly and surface plasmon resonance peaks at 445 nm indicated the successful formation of Fd-AgNPs. Dynamic light scattering and zeta potential revealed that Fd-AgNPs possess an average hydrodynamic size of 120.4 nm with monodispersity and good stability. X-ray diffraction patterns exhibited (111), (200), (220), (311) reflection peaks, confirming its face-centered cubic crystalline structure. In antimicrobial evaluations, disk diffusion tests demonstrated that Fd-AgNPs possessed intrinsic antibacterial activity comparable to $AgNO_3$. While ampicillin alone exhibited stronger inhibitory potency against *S. aureus* than *E. coli*, kanamycin and streptomycin displayed equivalent zones of inhibition across both pathogens. Crucially, checkerboard assays revealed a profound synergistic effect with Fd-AgNPs combining with kanamycin and streptomycin, resulting in 31-fold and 4-fold reductions in their minimum inhibitory concentrations, respectively. Overall, this study demonstrates that *F. deltoidea*-mediated AgNPs possess ideal physicochemical properties and offer promising adjuvant therapy to reduce antibiotic dosages and enhance their antibacterial potency in the post-antibiotic era.
Keywords: Silver nanoparticles; *Ficus deltoidea*; conventional antibiotics; antibacterial assays; synergistic antibacterial

Introduction

Antibiotics profoundly revolutionized modern medicine, but the concurrent rise in antimicrobial resistance (AMR) due to indiscriminate use, combined with the slow pace of novel drug development, has created a pressing global public health crisis (Chi et al., 2025; WHO, 2019). Historically, antibacterial discovery relied on narrow targets like bacterial cell walls and ribosomes, which have been extensively mined (Theuretzbacher et al., 2023). Formidable barriers such as impermeable envelopes, efflux pumps, rapid gene mutations, and economic bottlenecks severely restrict novel antibiotic engagement (Galgano et al., 2025; Gargate et al., 2025; Miethke et al., 2021). Consequently, silver nanoparticles (AgNPs) have emerged as a promising alternative, exerting broad-spectrum activity through multi-targeted mechanisms, such as cell envelope disruption and reactive oxygen species (ROS) generation to bypass single-agent resistance (Khalifa et al., 2025).

Unlike physical and chemical synthesis methods that suffer from high energy consumption and toxic reagents, plant-mediated green synthesis offers an eco-friendly, cost-effective alternative (Barros et al., 2018). Bioactive phytochemicals in botanical sources act as dual-functional reducing and capping agents, enabling stable nanoparticle formation without synthetic surfactants. Among these, *Ficus deltoidea* possesses high antioxidant potential for biogenic AgNP fabrication. Furthermore, combining biogenic AgNPs with conventional antibiotics can lower minimum inhibitory concentrations (MICs) and achieve synergistic antibacterial effects (Keshari et al., 2020). Although previous studies evaluated the individual antibacterial activity of *F. deltoidea*-mediated AgNPs using disk diffusion and microdilution

assays (Din et al., 2022), a critical research gap remains: the potential synergistic interactions between *F. deltoidea*-derived AgNPs and conventional antibiotics have not yet been systematically investigated.

To address this gap, this study aims to synthesize and characterize *F. deltoidea*-biosynthesized AgNPs, evaluate the individual antibacterial activities of AgNPs and three conventional antibiotics, and systematically investigate the antibacterial efficacy of their combination against Gram-negative *Escherichia coli* (ATCC 11229) and Gram-positive *Staphylococcus aureus* (ATCC 29213). Synthesis parameters were optimized via a one-factor-at-a-time approach, and the resulting AgNPs were characterized using visible spectrophotometry, dynamic light scattering, zeta potential, and X-ray diffraction. Following preliminary disk diffusion tests and quantitative MIC determinations via microdilution assays, a 96-well checkerboard assay was employed to evaluate combination behaviors using the fractional inhibitory concentration index (FICI). This research advances green chemistry and offers a viable, low-cost strategy to restore antibiotic potency, reduce required dosages, and mitigate the post-antibiotic crisis of antimicrobial resistance.

Materials and methods

F. deltoidea was purchased from Juaseh Tengah, Negeri Sembilan, Malaysia, and cultivated for 4 years prior to harvest. Sliced plant materials were rinsed with deionized (DI) water and dried at 40 °C overnight (Azizah et al., 2025). The dried biomass was pulverized using a mechanical blender, passed through a 104-mesh sieve, and stored at 4 °C. For extract preparation, 2 g of powdered biomass was suspended in 100 mL of freshly boiled DI water (2% w/v) and stirred at 100 °C for 30 min on a magnetic hotplate. The mixture was cooled to 25 °C, filtered through Whatman No. 1 filter paper, and the filtrate was preserved at 4 °C (Permatasari et al., 2026; Azizah et al., 2025).

Reaction parameters were optimized using a one-factor-at-a-time (OFAT) strategy in triplicate to ensure consistent physicochemical properties. Initially, *F. deltoidea* extracts at concentrations of 0.1%, 0.5%, 1.0%, 1.5%, and 2.0% (w/v) were prepared. Each extract variant of 5 mL was mixed with 10 mL of 1 mM $AgNO_3$ solution and incubated at ambient temperature for 24 h. AgNPs formation was monitored visually by color change and measured over the 350 – 800 nm range using a Jenway 7200 Visible Spectrophotometer. The $AgNO_3$ concentration gradient was set at 0.1, 0.5, 1.0, 1.5, and 2.0 mM. Lastly, the ratios of optimal plant extract to optimal AgNO3 solution were set to 1:1, 1:2, 1:5, 1:10, and 1:15.

With the optimal reaction conditions established, lab-scale production of AgNPs was carried out in a 1 L round-bottom flask. The reaction mixture was incubated for 1 day at 25°C. The synthesized AgNPs were centrifuged at 9,500 rpm for 10 mins. The collected AgNPs pellets were completely dried at 60°C in an oven for 24 hours. Visible spectrophotometry was employed to observe Surface Plasmon Resonance (SPR) and confirm the successful synthesis, Dynamic Light Scattering and Zeta Potential for size distribution and colloidal stability, and finally X-ray Diffraction (XRD) to confirm the crystal structure.

Before performing the disk diffusion test, both *E. coli* and *S. aureus* were cultured and incubated. A bacterial suspension was prepared and adjusted to a 0.5 McFarland standard. This standard corresponded to a bacterial turbidity of approximately 1.5×10^8 CFU/mL. For each bacterial strain, one mueller hinton agar (MHA) plates contained a blank paper disc loaded with deionized water as a negative control, a disc loaded with plant extract, a disc loaded with 1 mM $AgNO_3$ solution, and a disc loaded with 1 μg/mL silver nanoparticles. The other dish contained three conventional antibiotics of 100 μg/mL. Each bacterial strain was tested in triplicate, resulting in a total of six petri dishes.

The MIC values for three individual antibiotics and AgNPs were determined using the microdilution method in 96-well plates, following the Clinical and Laboratory Standards Institute (CLSI) guidelines (Alotaibi et al., 2022). Each treatment well was composed of 100 µL of bacterial inoculum, 50 µL of AgNPs colloidal solution or certain antibacterial reagent and 50 µL of distilled water. All antibacterial solutions were prepared via serial two-fold dilution of the stock solution and the bacterial suspension was adjusted to the 0.5 McFarland standard. Subsequently, the standardized suspension was diluted in Mueller-Hinton Broth (MHB, Oxoid, UK) to a final density of 10^6 CFU/well. The optimally synthesized AgNPs were collected by centrifugation at 9,500 rpm for 10 min. Approximately three-

quarters of the supernatant was carefully removed, and the remaining suspension was resuspended to obtain a concentrated AgNPs colloidal stock solution. Antibiotic stock concentrations were selected based on CLSI breakpoints, and dilutions ranged to cover both susceptible and resistant strains (CLSI, 2015). Experimental controls comprised blank (200 µL uninoculated MHB), positive (200 µL pure ethanol), and negative (100 µL bacterial suspension and 100 µL distilled water) wells. The plates were incubated for 16 hours at 37 °C. 10 µL of resazurin reagent was added to each well for 2-hour incubation at 37 °C. The MIC was defined as the lowest concentration preventing the resazurin color change from blue to pink or slight purple.

A checkerboard assay was carried out in 96-well plates using a two-dimensional serial dilution strategy. AgNPs were serially diluted twofold along the vertical axis, spanning concentrations from MIC to 1/64 × MIC. Similarly, each antibiotic was added in two-fold serial dilutions horizontally, covering the concentration range from MIC to 1/128 × MIC. Each well contained a pair of AgNPs concentrations and a specific antibiotic, along with a bacterial inoculum, resulting in a final volume of 200 µL. The plates were incubated at 37 °C for 16 hours. Bacterial viability was assessed using a resazurin-based colorimetric assay after incubation. The fractional inhibitory concentration index (FICI) was calculated as follows:

$$FICI = \left(\frac{MIC_{combination_{AgNP}}}{MIC_{alone_{AgNP}}}\right) + \left(\frac{MIC_{combination_{Antibiotic}}}{MIC_{alone_{Antibiotic}}}\right)$$

The interactions are interpreted as synergistic (FICI ≤ 0.5), additive (0.5 < FICI ≤ 1), indifferent (1< FICI ≤ 4), or antagonistic (FICI > 4).

Results and discussion

As shown in Figure 1, nanosilver formation was visually confirmed by a color shift from nearly transparent to deep red. Increasing the silver nitrate concentration up to 1.5 mM continuously enhanced the surface plasmon resonance peak intensity to its maximum, whereas 0.1 mM showed no visible peak due to insufficient yield, as noted by Chandraker et al. (2021). The decline in absorbance at 2.0 mM without peak broadening indicates partial precipitation from insufficient reducing agents rather than severe aggregation, establishing 1.5 mM as the optimal precursor concentration.

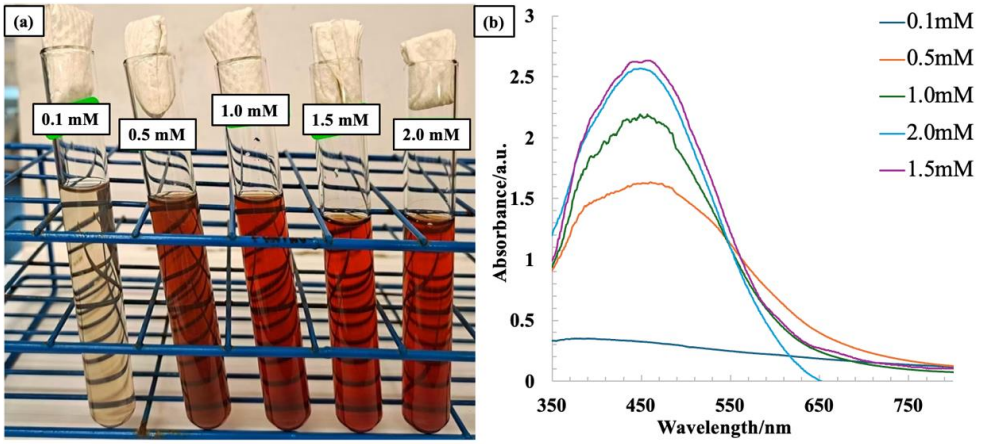

Figure 1 Colour intensity (a) of synthesized AgNPs using different concentrations of $AgNO_3$ and Visible Spectra (b) of AgNPs at different $AgNO_3$ concentrations

Figure 2 demonstrates that increasing the plant extract concentration from 0.1% to 1.5% weight by volume produced a strong hyperchromic effect, beyond which the absorption spectra plateaued due to reaction equilibrium, as reported by Rahman et al. (2024). The surface plasmon resonance bands narrowed up to 1.5% and remained consistently centered between 440 and 450 nm, confirming improved size uniformity and core particle stability without significant size shifts.

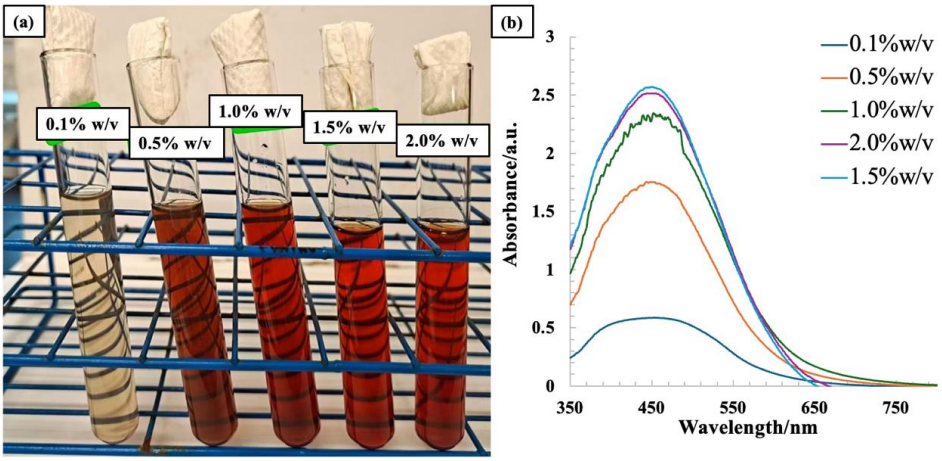

Figure 2 Colour intensity (a) of synthesized AgNPs using different concentrations of *F. deltoidea* and Visible Spectrum (b) of AgNPs at different plant extract Concentrations

As depicted in Figure 3, increasing the extract-to-precursor volume ratio from 1:1 to 1:5 sharply elevated peak absorbance to approximately 4.3 arbitrary units (a.u.) due to accelerated nucleation kinetics (Ansari et al., 2023). Further increasing the ratio to 1:10 and 1:15 caused absorbance to drop and peaks to broaden due to insufficient phytochemical capping and particle agglomeration, establishing 1.5 mM precursor, 1.5% weight by volume extract, and a 1:5 ratio as the optimal parameters.

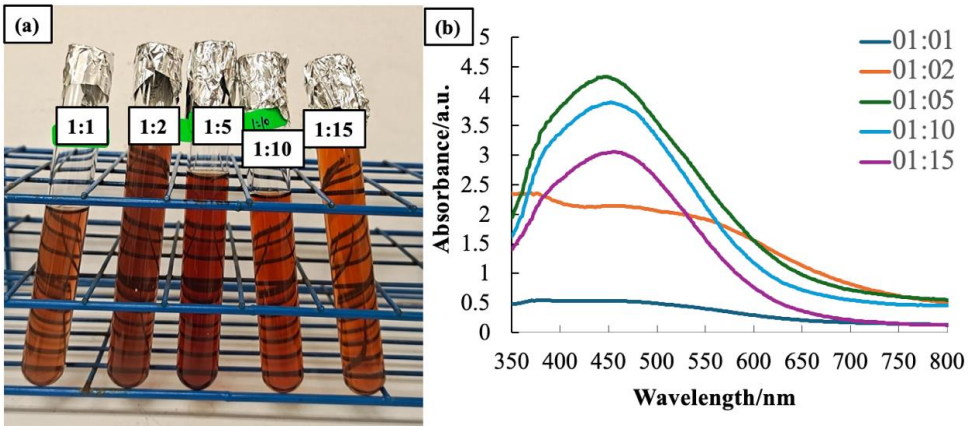

Figure 3 Colour Intensity (a) of synthesized AgNPs using different volume ratio between plant extract and $AgNO_3$ and Visible Spectrum (b) of AgNPs at different volume ratios between plant extract and $AgNO_3$

The characteristic surface plasmon resonance band centered at 445 nm confirms the successful formation of AgNPs after optimization, consistent with the complete silver ion reduction reported by Malek et al. (2023). A high peak absorbance of ~4.33 a.u. indicates excellent conversion efficiency and yield within the colloidal solution. Furthermore, the narrow, symmetrical peak profile reflects a narrow size distribution and good monodispersity among the biosynthesized nanoparticles (Rahman et al., 2019; Rolim et al., 2019).

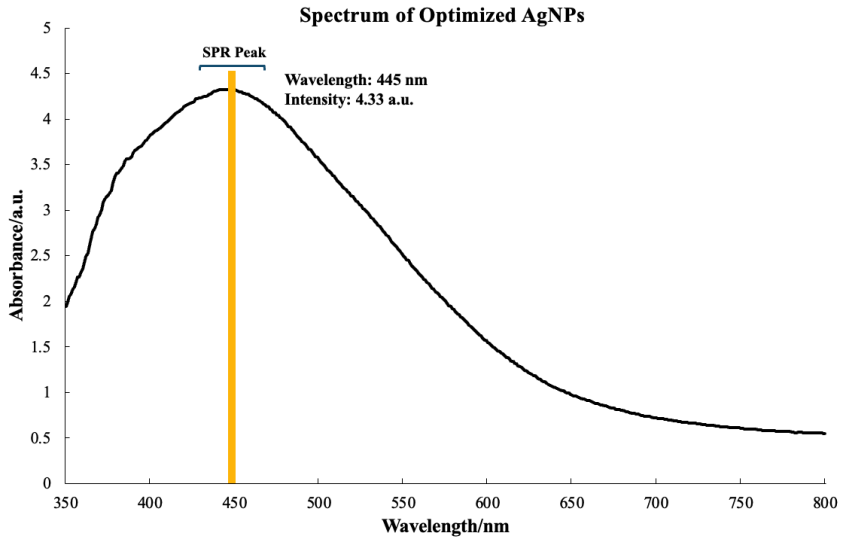

Figure 4 Visible Spectrum of AgNPs synthesized under the optimized reaction conditions.

Dynamic light scattering analysis revealed that the synthesized Fd-AgNPs exhibited an average hydrodynamic diameter of 109.8 – 131 nm with low polydispersity index (PDI) values of 0.219 – 0.230 as shown in Figure 5. A PDI below 0.3 confirms a narrow size distribution and desirable monodispersity (Bhattacharjee, 2016). This is further supported by the size distribution profile, which displays a unimodal peak with 100% intensity, verifying the absence of large agglomerates in the colloidal suspension (Stetefeld et al., 2016).

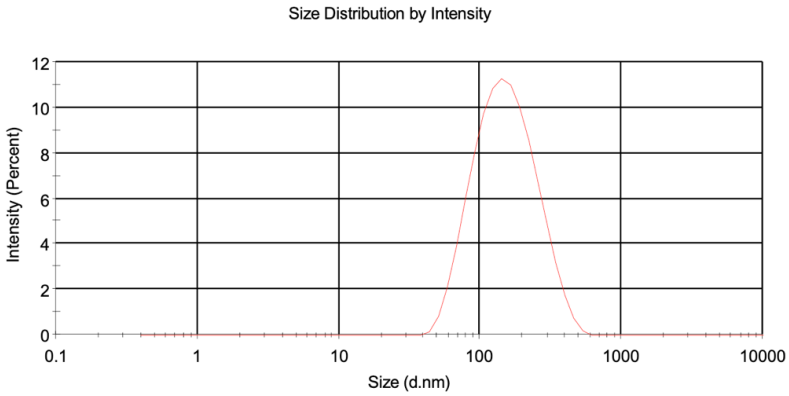

Figure 5 Size distribution by intensity of Fd-AgNPs

The physicochemical properties of the synthesized Fd-AgNPs, including their hydrodynamic size, polydispersity, and surface charge, are summarized in Table 1.

Table 1: Physicochemical characterization of Fd-AgNPs including Hydrodynamic Diameter, PDI, Zeta-potential, and Peak 1 intensity.

Sample	Hydrodynamic Diameterc(nm)	PDI	Zeta-Potential (mV)
Fd-AgNPs	120.4 ± 10.6	0.223 ± 0.006	-2.95 ± 0.1

Regarding the surface charge, the zeta potential of the Fd-AgNPs was measured to be approximately -3.0 mV, with a range of -2.84 to -3.02 mV.

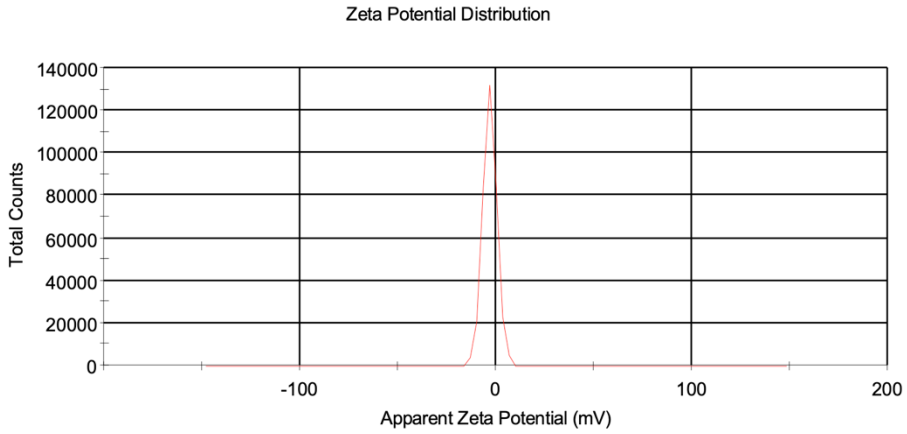

Figure 6 Zeta Potential Distribution of Fd-AgNPs

Although electrostatic stabilization typically requires a zeta potential magnitude above 30 mV (Malvern Instruments, 2011), the synthesized Fd-AgNPs remained uniformly dispersed despite a low zeta potential. This indicates that colloidal stability was governed primarily by steric hindrance rather than electrostatic repulsion (Lima et al., 2020). Phytochemicals and biological macromolecules from the *Ficus deltoidea* extract serve as capping agents, forming a spatial barrier around the nanoparticles to prevent aggregation (Das et al., 2021; Keshari et al., 2020; Shaikh et al., 2021; Zuhrotun et al., 2023). This finding aligns with Azizah et al. (2026), who similarly reported stable Fd-AgNPs at a low zeta potential (~ –1.2 mV) due to steric stabilization provided by secondary botanical metabolites.

As shown in Figure 7, the XRD pattern of Fd-AgNPs exhibited prominent Bragg reflections at 2θ values of 38°, 44°, 64°, and 77°, indexing to the (111), (200), (220), and (311) planes of face-centered cubic metallic silver (ICDD card 04-0783) (Asif et al., 2022; Waiezi et al., 2023). Applying the Debye–Scherrer equation to the dominant (111) peak yielded an average crystallite size of 10 – 10.6 nm (Permatasari et al., 2025). Minor peak shifts were attributed to surface lattice strain induced by phytochemical capping (Waiezi et al., 2023). Additionally, low-intensity secondary peaks at 27°, 32°, 46°, 54°, and 57°, confirmed the co-existence of a minor silver chloride (AgCl) phase (ICDD card 00-031-1238), a common occurrence in plant-extract-mediated synthesis (Permatasari et al., 2025).

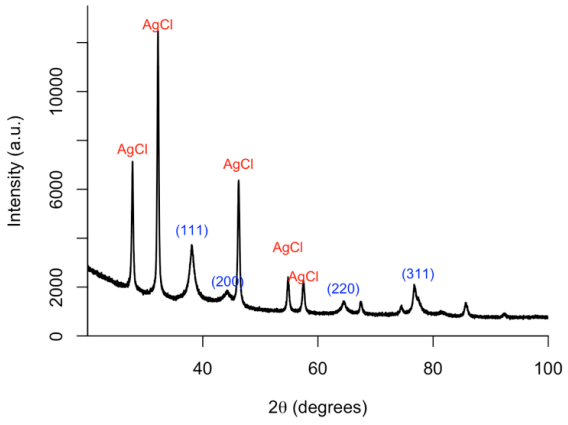

Figure 7: X-ray diffraction pattern of the biosynthesized Fd-AgNPs. The prominent Bragg reflections at 2θ values correspond to the (111), (200), (220), (311), and (222) planes of the face-centred cubic crystal structure of silver.

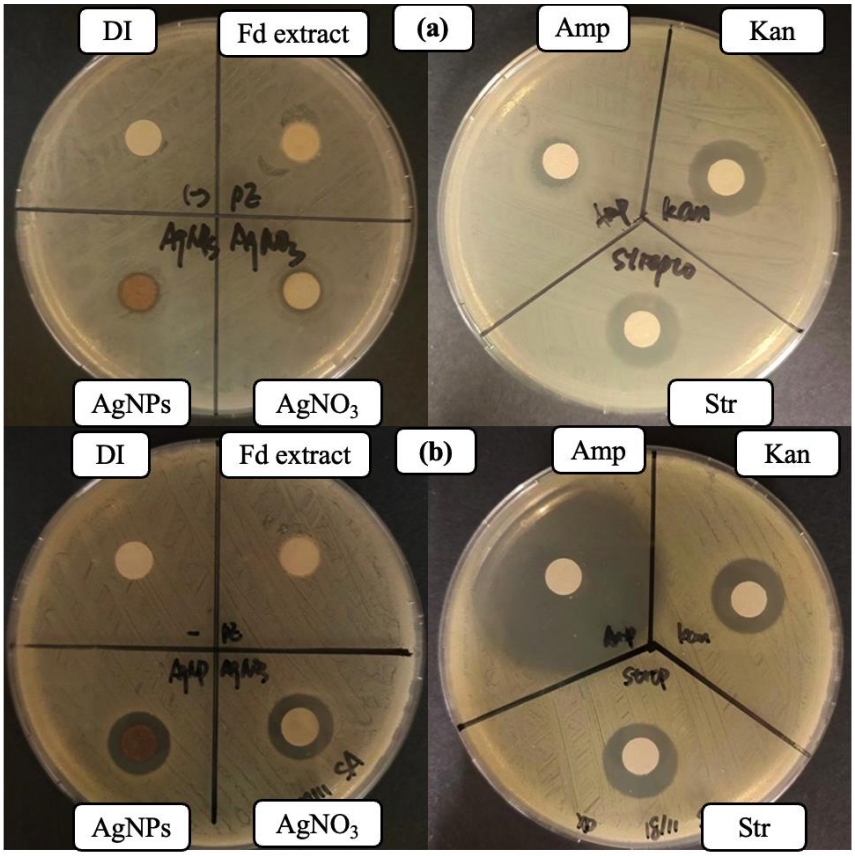

Figure 8: Images of DDT results against (a) *E. coli* and (b) *S. aureus*.

Table 2: DDT results of plant extracts, negative controls, biosynthesized AgNPs, and three antibiotics (ampicillin, kanamycin, and streptomycin) against *E. coli* and *S. aureus*.

Type of Sample	Concentration	Zone of Inhibition (mm)	
		E. coli	***S. aureus***
Negative Control	Deionized water	None	None
Plant Extract	2% w/v	None	None
Silver Nitrate	1mM	9.7 ± 0.6	13.7 ± 0.6
AgNPs	100 µg/mL	9.3 ± 0.6	12.7 ± 0.6
Ampicillin	100 µg/mL	9.7 ± 0.6	41.3 ± 1.5
Kanamycin	100 µg/mL	17 ± 0	18 ± 1
Streptomycin	100 µg/mL	16.7 ± 0.6	17 ± 1

As presented in Figure 8 and Table 2, neither the negative control nor the 2% w/v plant extract exhibited a zone of inhibition (ZOI), confirming that antibacterial activity originates solely from the Fd-AgNPs and their sustained silver ion release. The $AgNO_3$ precursor generated slightly larger ZOIs than Fd-AgNPs, reflecting direct ion availability. Fd-AgNPs exhibited broad-spectrum antibacterial activity against both pathogens; unexpectedly, a larger ZOI was formed against Gram-positive *S. aureus* than Gram-negative *E. coli*. While Gram-negative strains are typically more vulnerable due to their thinner cell wall (Vazquez-Muñoz et al., 2019), this inverse trend suggests specific surface interactions with the thick peptidoglycan layer of *S. aureus* or higher intrinsic resistance in the tested *E. coli* strain (Dakal et al., 2016).

Regarding conventional antibiotics, ampicillin displayed markedly higher efficacy against *S. aureus* than *E. coli*, consistent with its primary mechanism targeting Gram-positive cell wall synthesis (Peechakara et al., 2023). In contrast, kanamycin and streptomycin exhibited comparable inhibitory

capability against both strains without significant selectivity. This uniform potency aligns with their shared mode of action as aminoglycosides, which disrupt protein synthesis at the 30S ribosomal subunit to induce secondary membrane disruption (Tevyashova et al., 2022; Webster et al., 2022).

Quantitative checkerboard assays demonstrated that AgNPs exerted a pronounced strain-dependent potentiating effect when combined with conventional antibiotics, as summarized in Table 3. Combining AgNPs with kanamycin exhibited exceptional synergistic action against *E. coli* as FICI equals to 0.282, drastically reducing the MIC of kanamycin from 6.25 µg/mL to 0.2 µg/mL while concurrently lowering the MIC of AgNPs from 12.5% to 3.125%. A strong synergistic interaction was likewise observed with streptomycin with FICI of 0.375, whereas ampicillin combinations displayed additive activity with FICI of 0.75. In contrast, against *S. aureus*, combinations with kanamycin and streptomycin produced only additive effects with both FICIs equaling to 0.75, reducing their respective MICs from 1.56 µg/mL and 0.78 µg/mL to 0.39 µg/mL. Furthermore, ampicillin exhibited an indifferent interaction against *S. aureus*, leaving the conjugated AgNP MIC unchanged at 12.5%.

Table 3: Synergistic, additive, and indifferent effects of silver nanoparticles combined with antibiotics against *E. coli* and *S. aureus*. The table presents the MIC values for individual agents and their combinations, along with the calculated FICs and interpretations of interactions.

Strains	Combina-tion	MIC (alone)		MIC (conjugated)		FICI	Interpre-tation
		Antibiotics (µg/mL)	AgNPs (%)	Antibiotics (µg/mL)	AgNPs (%)		
E. coli	Amp + AgNPs	100	12.5	50	3.125	0.75	Additive
	Kan + AgNPs	6.25		0.2		0.282	Synergi –stic
	Str + AgNPs	3.125		0.78		0.375	Synergi s-tic
S. aureus	Amp + AgNPs	0.78	12.5	0.39	6.25	1.5	Indiffere -nt
	Kan + AgNPs	1.56				0.75	Additive
	Str + AgNPs	0.78					Additive

These results highlight that biosynthesized AgNPs serve as highly potent antibiotic adjuvants, exhibiting greater therapeutic efficacy against Gram-negative bacteria than Gram-positive strains. By significantly lowering the required dosage of conventional antibiotics, this combined administration strategy effectively minimizes off-target drug toxicity and offers a highly promising therapeutic approach to combat antimicrobial resistance.

Conclusion

In this study, optimized green synthesis using *Ficus deltoidea* extract successfully produced crystalline AgNPs under optimized conditions of 1.5% (w/v) extract concentration, 1.5 mM $AgNO_3$, and a 1:5 precursor-to-extract ratio. The synthesized nanoparticles exhibited a characteristic SPR peak at approximately 445 nm, face-centered cubic crystalline structure, and narrow particle size distribution with hydrodynamic diameters ranging from 108 to 128 nm and PDI values of 0.22 – 0.23. Despite their low zeta potential of approximately −3.0 mV, phytochemical capping contributed to nanoparticle stability. Antibacterial assessment demonstrated that AgNPs enhanced the efficacy of selected antibiotics in a strain-dependent manner, with kanamycin- and streptomycin-loaded AgNP combinations showing synergistic effects against *E. coli*, while predominantly additive interactions were observed against *S. aureus*. Importantly, this study successfully quantified the antibacterial efficacy of each AgNP + antibiotic combination against *S. aureus* and *E. coli* and determined the effective concentrations of each antimicrobial component within the combinations. This research provides useful reference data

for the future development of AgNPs-assisted antimicrobial therapies and combination treatment strategies.

Acknowledgement

The authors would like to express their appreciation to Dr. Nik Ahmad Nizam Nik Malek for his valuable supervision and guidance throughout this study. The authors also acknowledge Universiti Teknologi Malaysia for providing the laboratory facilities and institutional support necessary for this research.

References

Alotaibi, A. M., Alsaleh, N. B., Aljasham, A. T., Tawfik, E. A., Almutairi, M. M., Assiri, M. A., Alkholief, M., & Almutairi, M. M. (2022). Silver Nanoparticle-Based Combinations with Antimicrobial Agents against Antimicrobial-Resistant Clinical Isolates. Antibiotics, 11(9), 1219. https://doi.org/10.3390/antibiotics11091219

Ansari, M., Ahmed, S., Abbasi, A., Khan, M. T., Subhan, M., Bukhari, N. A., Hatamleh, A. A., & Abdelsalam, N. R. (2023). Plant mediated fabrication of silver nanoparticles, process optimization, and impact on tomato plants. Scientific Reports, 13(1), 18048. https://doi.org/10.1038/s41598-023-45038-x

Asif, M., Yasmin, R., Asif, R., Ambreen, A., Mustafa, M., & Umbreen, S. (2022). Green Synthesis of Silver Nanoparticles (AgNPs), Structural Characterization, and their Antibacterial Potential. Dose-Response, 20(2). https://doi.org/10.1177/15593258221088709

Azizah, J. S., Ngabdi, C. K., Fatiha, R. A., To, S. W., Malek, N. A. N. N., Riawan, W., Holipah, H., Sulistomo, H. W., Lestari, B., & Permatasari, H. K. (2026). Physicochemical characterization and anticancer potential of Ficus deltoidea-silver nanoparticles (FD-AgNPs) on HeLa cells: Evidence from apoptosis and proliferation assays. Biochemical and Biophysical Research Communications, 808, 153407. https://doi.org/10.1016/j.bbrc.2026.153407

Barros, C. H. N., Fulaz, S., Stanisic, D., & Tasic, L. (2018). Biogenic Nanosilver against Multidrug-Resistant Bacteria (MDRB). Antibiotics, 7(3), 69. https://doi.org/10.3390/antibiotics7030069

Bhattacharjee, S. (2016). DLS and zeta potential – What they are and what they are not? Journal of Controlled Release, 235, 337–351. https://doi.org/10.1016/j.jconrel.2016.06.017

Chandraker, S. K., Lal, M., Dhruve, P., Singh, R. P., & Shukla, R. (2021). Cytotoxic, Antimitotic, DNA Binding, Photocatalytic, H2O2 Sensing, and Antioxidant Properties of Biofabricated Silver Nanoparticles Using Leaf Extract of Bryophyllum pinnatum (Lam.) Oken. Frontiers in Molecular Biosciences, 7. https://doi.org/10.3389/fmolb.2020.593040

Chi, J., Lin, Q., Jin, B., Ou, J., Jiang, L., Yang, X., Guo, J., Peng, T., & Lu, C. (2025). Combating the post-antibiotic era crisis: antimicrobial peptide/peptidomimetic-integrated combination therapies and delivery systems. Journal of Materials Chemistry B, 13(38), 11996–12019. https://doi.org/10.1039/D5TB01424G

Dakal, T. C., Kumar, A., Majumdar, R. S., & Yadav, V. (2016). Mechanistic Basis of Antimicrobial Actions of Silver Nanoparticles. Frontiers in Microbiology, 7. https://doi.org/10.3389/fmicb.2016.01831

Das, S., Langbang, L., Haque, M., Belwal, V. K., Aguan, K., & Singha Roy, A. (2021). Biocompatible silver nanoparticles: An investigation into their protein binding efficacies, anti-bacterial effects and cell cytotoxicity studies. Journal of Pharmaceutical Analysis, 11(4), 422–434. https://doi.org/10.1016/j.jpha.2020.12.003

Din, S. M., Malek, N. A. N. N., Shamsuddin, M., Matmin, J., Hadi, A. A., & Asraf, M. H. (2022). Antibacterial silver nanoparticles using different organs of Ficus deltoidea Jack var. kunstleri (King) Corner. Biocatalysis and Agricultural Biotechnology, 44, 102473. https://doi.org/10.1016/j.bcab.2022.102473

Galgano, M., Pellegrini, F., Catalano, E., Capozzi, L., del Sambro, L., Sposato, A., Lucente, M. S., Vasinioti, V. I., Catella, C., Odigie, A. E., Tempesta, M., Pratelli, A., & Capozza, P. (2025). Acquired Bacterial Resistance to Antibiotics and Resistance Genes: From Past to Future. Antibiotics, 14(3), 222. https://doi.org/10.3390/antibiotics14030222

Gargate, N., Laws, M., & Rahman, K. M. (2025). Current economic and regulatory challenges in developing antibiotics for Gram-negative bacteria. Npj Antimicrobials and Resistance, 3(1), 50. https://doi.org/10.1038/s44259-025-00123-1

Ismail, I. Q., Nik Malek, N. A. N., Sani, N. S., Mohammad Din, S., & Asraf, M. H. (2023). Green Biosynthesized Silver Nanoparticles using Ficus deltoidea Leaf Extract as Antibacterial Agent. Bioresources and Environment, 1(3), 27–44. https://doi.org/10.24191/bioenv.v1i3.34

Keshari, A. K., Srivastava, R., Yadav, S., Nath, G., & Gond, S. K. (2020). Synergistic activity of green silver nanoparticles with antibiotics. Nanomedicine Research Journal, 5(1), 44–54. https://doi.org/10.22034/NMRJ.2020.01.006

Khalifa, H. O., Oreiby, A., Mohammed, T., Abdelhamid, M. A. A., Sholkamy, E. N., Hashem, H., & Fereig, R. M. (2025). Silver nanoparticles as next-generation antimicrobial agents: mechanisms, challenges, and innovations against multidrug-resistant bacteria. Frontiers in Cellular and Infection Microbiology, 15. https://doi.org/10.3389/fcimb.2025.1599113

Lima, A. K. O., Vasconcelos, A. A., Kobayashi, R. K. T., Nakazato, G., Braga, H. de C., & Taube, P. S. (2021). Green synthesis: characterization and biological activity of silver nanoparticles using aqueous extracts of plants from the Arecaceae family. Acta Scientiarum. Technology, 43, e52011. https://doi.org/10.4025/actascitechnol.v43i1.52011

Malvern Instruments. (2011). Zeta Potential: An Introduction in 30 Minutes. Technical Note MRK1510-01. Malvern, UK: Malvern Instruments Ltd.

Miethke, M., Pieroni, M., Weber, T., et al. (2021). Towards the sustainable discovery and development of new antibiotics. Nature Reviews Chemistry, 5, 726–749. https://doi.org/10.1038/s41570-021-00313-1

Peechakara, B. V., B. H., & G. M. (2023). Ampicillin. In StatPearls. StatPearls Publishing.

Permatasari, H. K., Firdaus, S. R. A., Susanto, H., Malek, N. A. N. N., Widodo, Holipah, & Sulistomo, H. W. (2025). Green synthesized Moringa oleifera Leaf Powder – Silver Nanoparticles (MOLP-AgNPs) promotes apoptosis by targeting Caspase-3 and Phosphorylated-AKT signaling in MCF-7 cells. Journal of Agriculture and Food Research, 19, 101640. https://doi.org/10.1016/j.jafr.2025.101640

Permatasari, H. K., Fatiha, R. A., Ngabdi, C. K., Azizah, J. S., Lestari, B., To, S. W., & Malek, N. A. N. N. (2026). Modulation of apoptotic pathways and epithelial–mesenchymal transition in HeLa cervical cancer cells by Ficus deltoidea-silver nanoparticles (FD-AgNPs). Phytomedicine Plus, 6(1), 100923. https://doi.org/10.1016/j.phyplu.2025.100923

Rahman, A., Kumar, S., Bafana, A., Dahoumane, S. A., & Jeffryes, C. (2018). Biosynthetic Conversion of Ag+ to highly Stable Ag0 Nanoparticles by Wild Type and Cell Wall Deficient Strains of Chlamydomonas reinhardtii. Molecules, 24(1), 98. https://doi.org/10.3390/molecules24010098

Rahman, M. U., Ullah, M. W., Alharbi, S. A., Alfarraj, S., Ul-Islam, M., Ali, M. Y., & Zhu, D. (2024). Development of a colorimetric sensor for selective manganese detection using green-synthesized silver nanoparticles from Withania somnifera. Results in Chemistry, 10, 101733. https://doi.org/10.1016/j.rechem.2024.101733

Rolim, W. R., Pelegrino, M. T., de Araújo Lima, B., Ferraz, L. S., Costa, F. N., Bernardes, J. S., Rodigues, T., Brocchi, M., & Seabra, A. B. (2019). Green tea extracts mediated biogenic synthesis of silver nanoparticles: Characterization, cytotoxicity evaluation and antibacterial activity. Applied Surface Science, 463, 66–74. https://doi.org/10.1016/j.apsusc.2018.08.203

Shaikh, W. A., Chakraborty, S., Owens, G., & Islam, R. U. (2021). A review of the phytochemical mediated synthesis of AgNP (silver nanoparticle): the wonder particle of the past decade. Applied Nanoscience, 11(11), 2625–2660. https://doi.org/10.1007/s13204-021-02135-5

Stetefeld, J., McKenna, S. A., & Patel, T. R. (2016). Dynamic light scattering: a practical guide and applications in biomedical sciences. Biophysical Reviews, 8(4), 409–427. https://doi.org/10.1007/s12551-016-0218-6

Tevyashova, A. N., & Shapovalova, K. S. (2021). Potential for the Development of a New Generation of Aminoglycoside Antibiotics. Pharmaceutical Chemistry Journal, 55(9), 860–875. https://doi.org/10.1007/s11094-021-02510-0

Theuretzbacher, U., Blasco, B., Duffey, M., & Piddock, L. J. v. (2023). Unrealized targets in the discovery of antibiotics for Gram-negative bacterial infections. Nature Reviews Drug Discovery, 22(12), 957–975. https://doi.org/10.1038/s41573-023-00791-6

Vazquez-Muñoz, R., Meza-Villezcas, A., Fournier, P. G. J., Soria-Castro, E., Juarez-Moreno, K., Gallego-Hernández, A. L., Bogdanchikova, N., Vazquez-Duhalt, R., & Huerta-Saquero, A. (2019). Enhancement of antibiotics antimicrobial activity due to the silver nanoparticles impact on the cell membrane. PLOS ONE, 14(11), e0224904. https://doi.org/10.1371/journal.pone.0224904

Waiezi, S., Malek, N. A. N. N., Asraf, M. H., & Sani, N. S. (2023). Preparation, Characterization, and Antibacterial Activity of Green-Biosynthesised Silver Nanoparticles using Clinacanthus nutans Extract. Biointerface Research in Applied Chemistry, 13(2). https://doi.org/10.33263/BRIAC132.171

Webster, C. M., & Shepherd, M. (2023). A mini review: environmental and metabolic factors affecting aminoglycoside efficacy. World Journal of Microbiology and Biotechnology, 39(1), 7. https://doi.org/10.1007/s11274-022-03445-8

World Health Organization. (2019). No time to wait: Securing the future from drug-resistant infections. Interagency Coordination Group on Antimicrobial Resistance (IACG). https://www.who.int/publications/i/item/no-time-to-wait-securing-the-future-from-drug-resistant-infections

Zuhrotun, A., Oktaviani, D. J., & Hasanah, A. N. (2023). Biosynthesis of Gold and Silver Nanoparticles Using Phytochemical Compounds. Molecules, 28(7), 3240. https://doi.org/10.3390/molecules28073240